A Glucose-Specific Metric to Assess Predictors and Identify Models

A Glucose-Specific Metric to Assess Predictors and Identify Models

Simone Del Favero, Andrea Facchinetti, and Claudio Cobelli*, *Fellow, IEEE*

***Abstract*—In diabetes, the mean square error (MSE) metric is extensively used for assessing glucose prediction methods and identifying glucose models. One limitation of this metric is that, by equally treating errors in hypo-, eu-, and hyperglycemia, it is not able to weight the different clinical impact of errors in these three situations. In this paper, we propose a new cost function, which overcomes this limitation and can be used in place of MSE for several scopes, in particular for assessing the quality of glucose predictors and identifying glucose models. The new metric called glucose-specific MSE (gMSE) modifies MSE with a Clark error grid inspired penalty function, which penalizes overestimation in hypoglycemia and underestimation in hyperglycemia, i.e., the most harmful conditions on a clinical perspective. From a mathematical point of view, gMSE retains sensitivity of MSE and inherits some of its important mathematical features, in particular it has no local minima, simplifying the optimization. This makes it suitable for model identification purposes also. First, the goodness of it is demonstrated by means of three experiments, designed ad hoc to evidence its sensitivity to accuracy, precision, and distortion in glucose predictions. Second, a prediction assessment problem is presented, in which two real prediction profiles are compared. Results show that the MSE chooses the worst clinical situation, while gMSE correctly selects the situation with less clinical risk. Finally, we also demonstrate that models identified minimizing gMSE are more accurate in potentially harmful situations (hypo- and hyperglycemia) than those obtained by MSE.**

***Index Terms*—Clark error grid (CEG), continuous glucose monitoring (CGM), diabetes, parameter estimation.**

I. Introduction

In the last few years, the diabetes management community has focused its attention on continuous glucose monitoring (CGM) sensors, noninvasive or minimally invasive portable devices, which allow HF readings (e.g., every 1–5 min) of glycemic concentration continuously for several days (up to 14) [1]–[3]. The availability of such a great amount of data opened the doors to the development of several applications devoted to the improvement of the quality of the diabetic patient's life, both for retrospective and real-time use [4]–[6]. In this paper, we will focus on two aspects, strongly connected one another: future glucose value prediction and model identification for model individualization.

Prediction of future glucose concentration, e.g., 30 min ahead in time, enables significant improvements in glycemic control. On patient's daily living, the combination of glucose prediction and an alert-generation system allows to timely prevent hypoglycemic (glucose ≤ 70 mg/dL) and hyperglycemic (glucose ≥ 180 mg/dL) episodes by warning patients of these possibly dangerous upcoming events and allowing a timely counteraction [7], [8]. Accurate prediction might also effectively benefit an automatic control device devoted to enforce tight glycemic control, i.e., the artificial pancreas. For instance, one of the most promising control techniques for this application is the so-called model predictive control, [9]–[11] and references therein, which chooses suitable control actions on the basis of its predicted effect on the patient. Prediction of glycemic changes as a consequence of insulin injection is especially needed in the artificial pancreas case since it mitigates for the large delay in the insulin action.

Model identification is the procedure that allows to estimate unknown parameters of a model on patient data. Physiological and data-driven models are widely used in diabetes clinical research, for instance, model is a crucial ingredient in model predictive controller for artificial pancreas. In view of large interindividual variability of physiological parameters, the use of individualized models obtained through model identification promises to be significantly more reliable than average models. Moreover, repeating the identification procedure on the same individual would enable to cope with the significant intraindividual variability, such as the day-by-day changes in the patient response to insulin. Models can be mechanistic/semimechanistic and, in this case, model identification reduces to the estimation of models parameters (white-box identification) [12], [13]. Alternatively, models can be black-box description of the system: polynomial [14], based on neural networks [15], [16], autoregressive [14], [17], or more general linear dynamical systems [18], and in this case, together with the parameter estimation, also the order selection has usually to be addressed [18].

Prediction and model identification are two very related issues. In the large majority of cases, future glucose concentrations are predicted on the basis of a model, desirably individualized on the patient. On the other hand, the quality of an identified model is assessed on the basis of its prediction capability. Moreover, as we will review later in Section II, the main-stream identification approach for black-box identification of a linear dynamical model is the so-called prediction error method that prescribes to estimate model's parameter so that the one-step-ahead prediction error is minimized in suitable norm, typically the mean square error (MSE).

Manuscript received September 21, 2011; revised December 15, 2011; accepted January 14, 2012. Date of publication January 23, 2012; date of current version April 20, 2012. *Asterisk indicates corresponding author.*

S. Del Favero and A. Facchinetti are with the Department of Information Engineering, University of Padova, 35131 Padova, Italy (e-mail: sdelfave@dei.unipd.it; facchine@dei.unipd.it).

*C. Cobelli is with the Department of Information Engineering, University of Padova, 35131 Padova, Italy (e-mail: cobelli@dei.unipd.it).

Color versions of one or more of the figures in this paper are available online at http://ieeexplore.ieee.org.

Digital Object Identifier 10.1109/TBME.2012.2185234

In training and model-test steps, the key role is played by the metric used. In glucose-related problems, standard metrics are usually used in both phases, for instance, MSE and other closely related metrics, such as fit and coefficient of determination (CoD) [19]. However, as we will illustrate in Section II, this choice is not always fully satisfactory in diabetes since different clinical risks are associated to the same absolute prediction error and this fact is not taken into account by standard cost functions. In the 1980s, when clinical accuracy of self-monitoring device was assessed to overcome this limitation, the so-called Clark error grid (CEG) was introduced [20], which is now a widespread clinical tool. Recently, CEG has also been applied to assess quality of prediction profiles from CGM data. However, as shown in [21], CEG is not suited for such a scope since it performs a too rough quantization to distinguish between similar profiles.

In this paper, we propose a new cost function with a two-fold purpose: first, to assess the accuracy of a predicted glucose profile on a clinical perspective (test phase), and second, to use it in place of the quadratic function in model identification (model-training phase). This is done suitably by penalizing the MSE cost to take into account specific diabetes issues, inspired by the CEG rationale. The proposed cost function retains sensitivity of MSE and inherits some of its important mathematical feature; in particular, it has no local minima, thus, simplifying the optimization. This makes the new cost suitable for model identification purposes.

The paper is organized as follow. In Section II, we review more deeply the relation between prediction and identification problem and introduce MSE. In Section III, we introduce the new metric, whose effectiveness is studied in Section IV on three conceptual experiments. In Section V, we illustrate a simple example of use of the new metric for prediction assessment, while in Section VI we present an example of model identification by minimizing the new cost function in place of the MSE. In Section VII, other prediction assessment metrics besides MSE are considered and in Section VIII we draw our conclusions. Finally, mathematical details are reported in Appendixes A and B.

II. Identification and Prediction Assessment: MSE

Prediction assessment and model identification are two strongly related issues. Indeed, most identification procedures estimate the parameter set that gives the most accurate prediction; hence, prediction assessment can be considered one step of the estimation routine. More precisely, the model identification problem can be formalized as follow.

Consider a model, i.e., a function f that returns an estimate of the blood glucose concentration $\hat{g}(t)$ on the basis of some measurable quantities that we collect in the vector $\Phi(t)$:

$$\hat{g}(t, \theta^*) = f(\Phi(t), \theta^*).$$

For instance, in a prediction case, $\hat{g}(t)$ is the blood glucose k steps ahead, while in $\Phi(t)$, we collect past blood glucose values and insulin injected. The model also depends on a parameter vector θ^*, unknown, that is specific to the patient and that we want to estimate with the model individualization procedure. The most common estimation procedure, the least square method, prescribes to estimate θ^* as follows:

$$\hat{\theta} = \min_{\theta} \text{MSE}(g(t), \hat{g}(t, \theta)) \quad (1)$$

$$\text{where} \qquad \text{MSE}(g(t), \hat{g}(t, \theta)) = \frac{1}{N} \sum_{t=1}^{N} (g(t) - \hat{g}(t, \theta))^2$$

i.e., $\hat{\theta}$ is chosen as the one that minimizes a suitable cost function that penalizes "bad" estimates. The least square approach penalizes the squared norm of the estimation Error (SE) $\text{SE} = (g(t) - \hat{g}(t, \theta))^2$ and therefore the cost function is known as MSE. This cost function has many advantages, the most important being the fact that it leads to closed-form solutions of the minimum problem in some relevant cases.

Still, in diabetes, this choice might be unsatisfactory since this standard metric does not take into account some clinically relevant facts, i.e., it penalizes in the same way errors that might have very different impact in diabetes therapy. For instance, from a clinical point of view, estimating $\hat{g}(t) = 80$ mg/dL when the actual blood glucose is $g(t) = 50$ mg/dL is a very harmful error since an hypoglycemic episodes are not detected. On the contrary, estimating $\hat{g}(t) = 50$ mg/dL when the the actual blood glucose is $g(t) = 80$ mg/dL is a much less dangerous error since it will lead to a likely not need hypotreatment. In an MSE context, these two situations have the same impact since they account only for the 30 mg/dL difference.

III. New Metric

In this section, we describe the new metric, *g*lucose-specific MSE, gMSE . Taking inspiration from the CEG [20], the MSE is suitably penalized to take into account specific diabetes issues. The resulting metric retains sensitivity and suitability to optimization as the MSE.

CEG was introduced to overcome limitations of MSE when assessing accuracy of self-monitoring devices [20]. The space of the couples of glucose reference values g and estimates obtained by self-monitoring $\hat{g}$, i.e., $(g, \hat{g})$, is divided in five regions, labeled from A to E, of increasing harmfulness, as shown in Fig. 1. Zone A corresponds to accurate estimation and Zone B corresponds to an inaccurate estimation with little effect on therapeutic decisions. Zone C leads to potentially dangerous over-treatment, for instance, an overbolus of insulin. On the contrary, in Zone D, severe hypo- or hyperglycemia episodes are not recognized, while data in Zone E are highly erroneous. Analogously, when assessing estimate quality, we want to penalize an overestimation in hypoglycemia and an underestimation in hyperglycemia, since in these cases, the actual risk is higher than the estimated one.

To this aim, we introduce a penalty function that, similarly to CEG, divides the $(g, \hat{g})$ space in three regions, of decreasing harmfulness.

1) Zone D1: $g \leq 70$ and $\hat{g} > g$. This is the maximally dangerous zone since an hypoglycemic episode is happening and we are overestimating the glucose concentration.
2) Zone D2: $g \geq 180$ and $\hat{g} < g$. Patient is hyperglycemic and we are underestimating the glucose concentration.

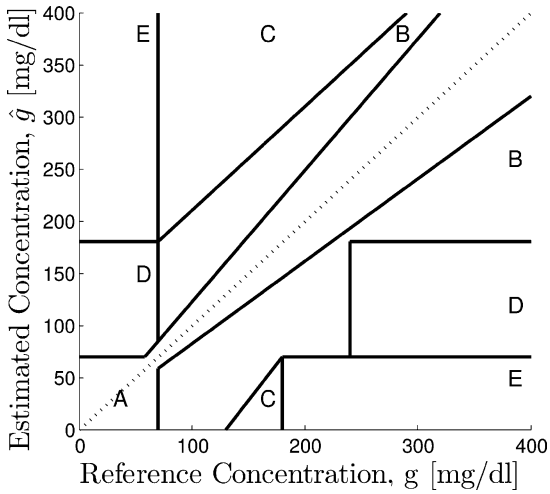

Fig. 1. Clark error grid.

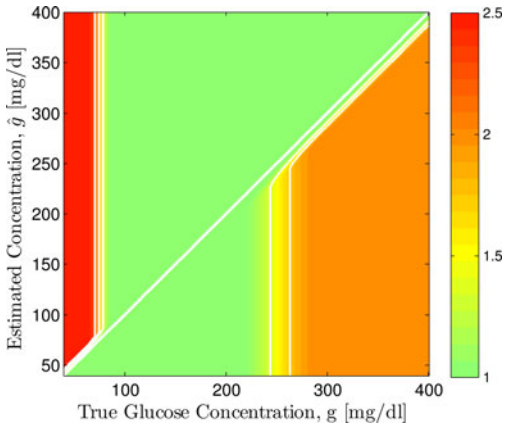

Fig. 2. Penalty function Pen in the $(g\,\hat{g})$ space.

3) Zone D3 covers the remaining part of the $(g, \hat{g})$ space. It includes the euglycemia region $70 \leq g \leq 180$, regardless of the estimate $\hat{g}$; the region in which the patient is hypoglycemic, $g \leq 70$, but the actual glycemia is underestimated ($\hat{g} < g$); and the analogous counterpart in the hyperglycemic region ($g > 180$ and $\hat{g} > g$), where an overestimation error occurs.

The penalty function will take the value 2.5 when $(g, \hat{g})$ is in zone D1, 2 when $(g, \hat{g})$ is in zone D2, and 1 when $(g, \hat{g})$ is in zone D3. Note that D2 penalty is lower than D1 because we associate a larger short-term risk to hypoglycemia.

As a second step, rather than dealing with a discontinuous and quantized penalty function, we consider its continuous approximation, $\text{Pen}(g, \hat{g})$, whose plot in the $(g, \hat{g})$ space is reported in Fig. 2. $\text{Pen}(g, \hat{g})$ is obtained substituting jumps with smooth sigmoid-like transitions $\sigma_{a,\epsilon}$ and $\bar{\sigma}_{a,\epsilon}$, as plotted in Fig. 3. Parameter a determines when the transition begins, while parameter ϵ determines the transition duration. $\text{Pen}(g, \hat{g})$ is defined as follows:

$$\text{Pen}(g, \hat{g}) = 1 + \alpha_L \bar{\sigma}_{g \leq T_L, \beta_L}(g) \sigma_{\hat{g} \geq g, \gamma_L}(\hat{g}, g) + \alpha_H \sigma_{g \geq T_H, \beta_H}(g) \bar{\sigma}_{\hat{g} \leq g, \gamma_H}(\hat{g}, g). \quad (2)$$

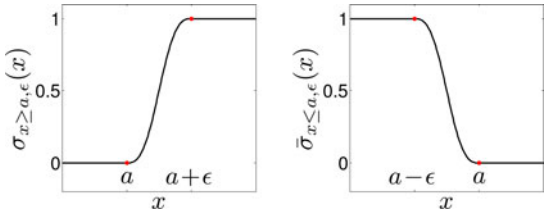

Fig. 3. Two sigmoid-like functions $\sigma_{x \geq a,\epsilon}(x)$ and $\bar{\sigma}_{x \leq a,\epsilon}(x)$.

TABLE I
VALUES OF THE PEN FUNCTION'S PARAMETERS

α_L	α_H	β_L	β_H	γ_L	γ_H	T_L	T_H
1.5	1	30	100	10	20	85	155

We chose $\alpha_L = 1.5$ and $\alpha_H = 1$ to approximate the discrete-valued penalty function's amplitude. $\beta_L, \beta_H, \gamma_L, \gamma_H$ are chosen, as reported in Table I, to have a fast change in the penalty function when entering in zone D1 and a more gradual change when entering in the less dangerous zone D2. The threshold $T_L = 85$ mg/dL is chosen to take into account the transient introduced by the smooth transition to zone $D1$. For instance, $\text{Pen}(85, 120) = 1$, therefore, not applying any extra penalty while $\text{Pen}(70, 120) = 1.75$ (since $\beta_L = 30$), hence, applying a moderate penalty for a mild hypoglycemia, and reaches the value of $\text{Pen}(g, 120) = 2.5$ for any $g < 55$ mg/dL (severe hypoglycemia). An analogous rationale suggested the choice of the threshold $T_H = 155$ mg/dL.

Finally, the new metric we propose is obtained by multiplying $\text{Pen}(g, \hat{g})$ times the quadratic function $SE(g, \hat{g})$:

$$gSE\,(g, \hat{g}) = SE(g, \hat{g})\text{Pen}(g, \hat{g}).$$

The new metric, glucose-specific square error, gSE, is therefore similar to the quadratic cost function but it has some extra penalties in the zones, where the error is potentially more dangerous from a clinical point of view, as in CEG. A plot of the new cost function is reported in Fig. 4(a). In Fig. 4(b), we also report the level curves of the gSE in the $(g, \hat{g})$ space, superimposed to the CEG. One can notice that the gSE can be seen as a continuous interpolation of the discrete valued CEG. Note in particular that the cost function grows very rapidly if an overestimation error is performed in the hypoglycemic region, while the increase is much slower if an underestimation error happens in the same region. Finally, it is to be noticed how the converse is true in the hyperglycemic region and how, in this case, the difference in the rate of increase is smaller as compared with the hypoglycemia case (considered more dangerous).

Remark: The choice of parameters in Table I has been done to achieve a good match between the level curves of the gSE and the CEG, see Fig. 4(b).

As for MSE, to evaluate with gSE the performance of an estimate versus reference profile, we simply take the average over time of gSE values obtained by point-to-point comparison

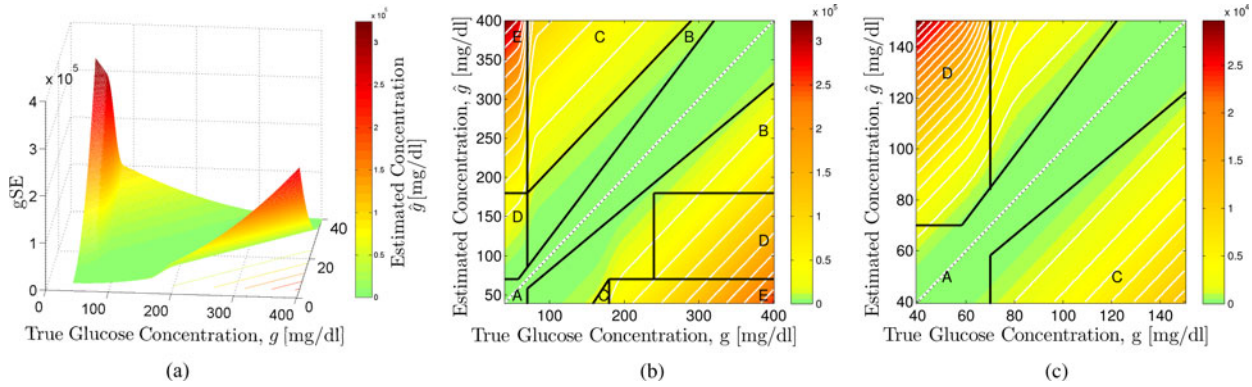

Fig. 4. (a) gSE cost function. (b) gSE level curves compared with CEG. (c) gSE versus CEG: zoom on the hypoglycemic region.

of the two time series:

$$\text{gMSE} = \frac{1}{N}\sum_{t} \text{gSE}(g(t), \hat{g}(t)).$$

Let us remark also that we have considered so far a "generic" estimate of the glucose concentration $\hat{g}$ that might be the one-step-ahead prediction but also any other PH steps ahead predictions or even the retrospective estimate obtained when future glucose concentrations become available.

As we remarked previously, within an identification procedure, the metric will be used as cost function in optimization problem. It is well known that a convex optimization problem is intrinsically easy and can be solved by using standard convex optimization techniques, while this is not the case for a nonconvex problem, the main issue being that an optimization algorithm may end up on a local minimum. For this reason, we are interested in studying convexity of the proposed metric.

To begin with, let us note that being the product of two $\mathcal{C}^2$ functions (see Appendix A), the $\text{gSE}(g, \hat{g})$ is $\mathcal{C}^2$ with respect to both variables.

The following results hold.

Proposition 3.1: Provided that $\alpha_H < 5$ and $\alpha_L < 5$ than

$$\frac{\mathrm{d}^2}{\mathrm{d}\hat{g}^2}\text{gSE}(g, \hat{g}) \geq 0.$$

Proof: Reported in Appendix B.

Corollary 3.1: The proposed cost function $\text{gSE}(g, \hat{g})$ is convex with respect to $\hat{g}$ for any true blood glucose value g.

Corollary 3.2: Being the sum of convex functions, also the cost $\text{gMSE}(g(t), \hat{g}(t))$ is convex with respect to the variables $\{\hat{g}(t)\}_t = 1, \ldots, N$, for any true blood glucose profile $\{\hat{g}(t)\}_t = 1, \ldots, N$.

In some relevant cases, the prediction $\hat{g}$ is a linear function of the parameters. For instance, this happens when performing black-box identification using AutoRegressive with eXogenous input (ARX) models. If this is the case, convexity of the metric ensures convexity of the optimization problem to be solved in the identification procedure.

Clearly, if prediction $\hat{g}$ is a nonlinear function of the parameters, convexity of the metric is not sufficient to guarantee convexity of the optimization problem. This happens when performing black-box identification using AutoRegressive Moving Average with eXogenous input (ARMAX) or Box Jenkins models [19]. However, in this case, optimizations is also nonconvex if MSE is used.

IV. gMSE Features

Three main points define the quality of a prediction method: precision, accuracy, and prediction distortion. Any metric oriented to prediction assessment and to model identification should finely distinguish predictions that are more precise/accurate/undistorted from those which are less precise/accurate/undistorted and recognize the first ones as better.

To test this, we propose three simple thought experiments, each of which is designed to test sensitivity to one of the issues mentioned previously, independently on the other and on the estimation method chosen.

Experiment 1 (Precision): The first conceptual experiment is used to evaluate the sensitivity of the metric to a zero-mean random error in the estimate. To isolate the effect of the noise, we assume that the estimated glucose $\hat{g}$ is simply a noisy version of the actual glucose $g(t)$:

$$\hat{g}(t) = g(t) + e(t) \tag{3}$$

where the estimation error $e(t)$ is a zero-mean independent identically distributed Gaussian process with variance

$$\text{Var}\big(e(t)\big) = \lambda^2.$$

An effective metric should finely distinguish between two different estimates, $\hat{g}_1$ and $\hat{g}_2$, with different error variance, λ_1 and λ_2.

In the diabetes applications, finer sensitivity is required when the patient is experiencing hypo- or hyperglycemia. To test the performance of our metrics on this point, we perform another experiment. True blood glucose g is now assumed to be constant in time:

$$g(t) = G \qquad \forall t$$

and we let G take different values. In Fig. 5, the cost function values are plotted against the estimation error variance for various G, namely, $G = [50,\ 70,\ 130,\ 200,\ 250,\ 300]$. Fig. 5(a) shows that MSE, being based only on the squared error norm, exhibits the same sensitivity to the noise regardless of the value of G, while on the contrary, the new cost gMSE is less sensitive in euglycemia while it becomes more and more sensitive as the true glucose value G moves toward the hypo- or hyperglycemic

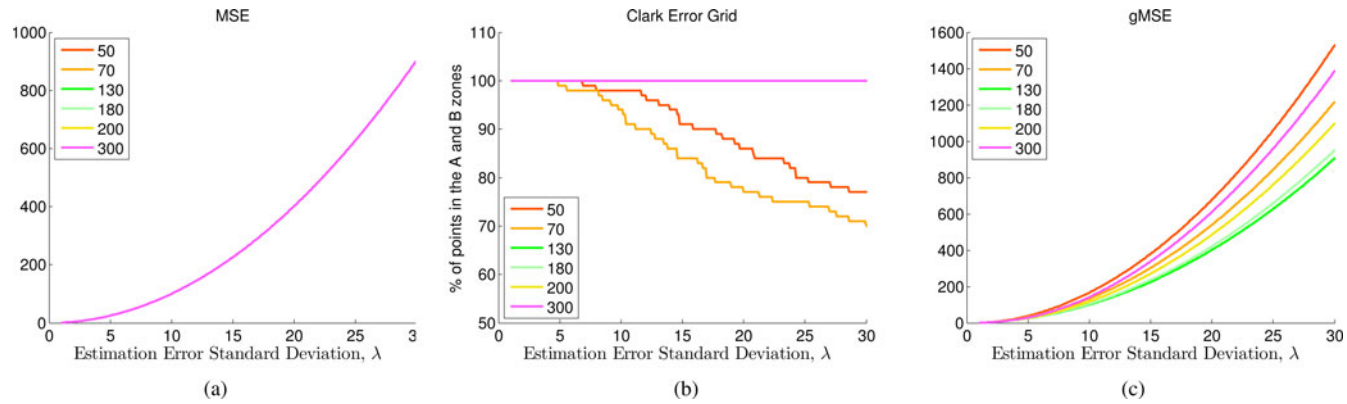

Fig. 5. Conceptual experiment 1. Plots of the cost function values against the estimation error variance for various values of the G.

regions [see Fig. 5(c)]. Note also that increment of sensitivity is faster as G enters in the hypoglycemic region with respect to G entering in the hyperglycemia region.

One might wonder if CEG itself can be used to assess the prediction, for instance, considering the percentage of points falling in the A zone, as it was done in [22] and [23]. Fig. 5(b) shows that CEG is insensitive to the noise, except for the case of very low or very high glycemia. It is also interesting to evidence that the sensitivity to the noise when $G = 50$ is lower than the one exhibited when $G = 70$. This undesirable effect is a consequence of the enlargement of region A for small glucose values. CEG was in fact built for a slightly different purpose and its straightforward application for prediction assessment might be ineffective or even misleading.

Experiment 2 (Accuracy): To be effective, a metric has to be able to penalize a bias in the estimate. Moreover, in view of diabetes application, also the sign of the bias has to be taken into account. The second conceptual experiment tests the metrics on this point. To isolate the effect of the bias, we assume that the estimate $\hat{g}(t)$ is exactly the true blood glucose concentration except for a constant estimation bias:

$$\hat{g}(t) = g(t) + B.$$

In this experiment, $g(t)$ is chosen as follows:

$$g(t) = G + 50\sin(2\pi t).$$

In Fig. 6, we plot the cost function values against the estimation basis B for various values of mean G. Fig. 6(b) is obtained for $G = 150$, i.e., $g(t)$ spans the range $[100,\ 200]$, remaining always in the euglycemic zone. Fig. 6(b) shows that MSE (blue line) finely distinguishes between different biases and that the same fine sensitivity is inherited by the gMSE (red line). Fig. 6(a) is obtained for $G = 100$, i.e., $g(t)$ spans the range $[50,\ 150]$ and hence it is often in the hypoglycemic zone. In this case, a positive bias $B > 0$ is very dangerous since it leads to underestimate a harmful episode while a negative bias $B < 0$ is less critical. MSE finely distinguishes between different biases but is unable to take into account the different harm of a positive bias and a negative bias, depending only on the bias' absolute value $|B|$. The new gMSE behaves like the quadratic cost function for positive biases $B > 0$ but grows much faster than the quadratic

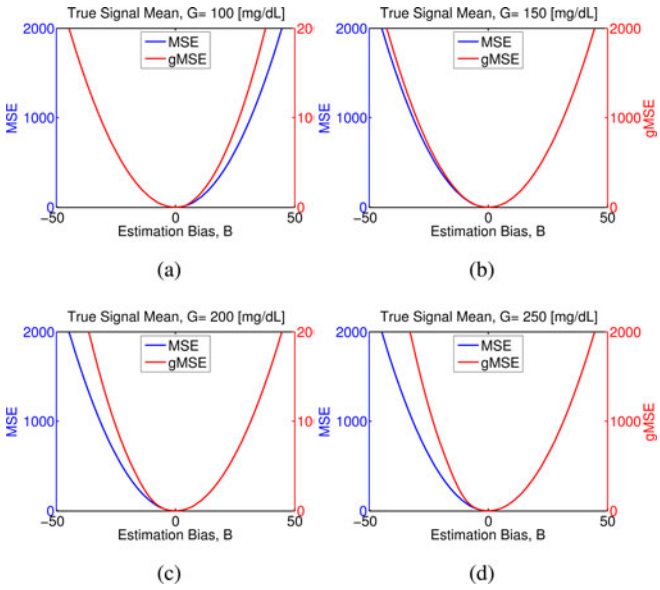

Fig. 6. Conceptual experiment 2. Plots of the cost function values against the estimation basis B for various values of the true signal mean G.

one for negative biases $B < 0$, thus, taking into account the impact of the bias' sign in the therapy. Analogous conclusions can be drawn looking at Fig. 6(c) and (d), obtained for $G = 200$ and $G = 250$, respectively, hence, with $g(t)$ spending significant time in hyperglycemic zone.

Experiment 3 (Distortions): The last thought experiment is designed to test the sensitivity of the metric to a distortion in the estimate. To this aim, we assume that the estimate $\hat{g}(t)$ is a distorted version of the actual blood glucose $g(t)$

$$\hat{g}(t) = d\big(g(t)\big)$$

where the distortion function $d(\cdot)$ is assumed as a simple, piecewise linear, static function, as the one reported in Fig. 7(a). The function $d(\cdot)$ describes the case of accurate estimates in the euglycemic region and inaccurate estimates in hypo- and hyperregions, where the signal is stretched of a fixed factor Δ_L and Δ_H, respectively, for instance, due lack of validation of the estimation model in these regions. Inaccuracy in the estimate might be also induced by a less reliable sensor reading in hypoglycemic zones, [24], [25].

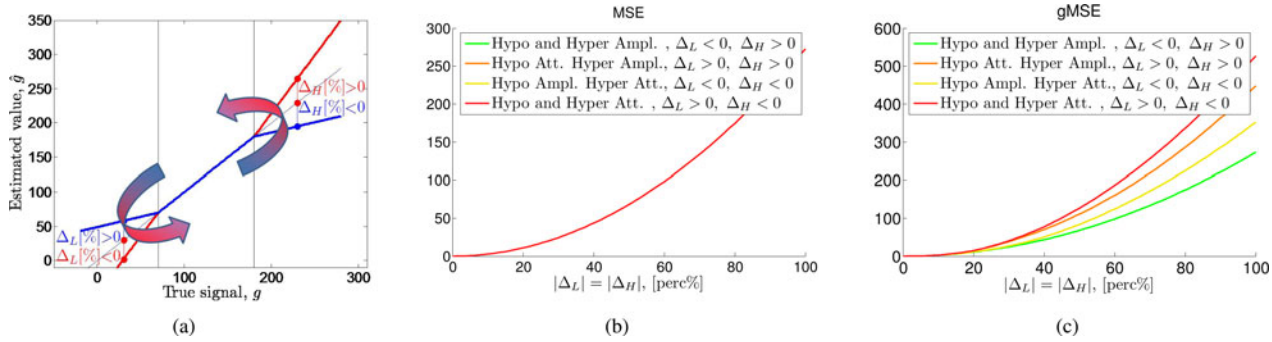

Fig. 7. Conceptual experiment 3. (a) Reports the distortion $d(\cdot)$ in the estimates $\hat{g}(t)$. In (b) and (c) are plotted the cost function values against the hypo- and hyperglycemic distortion Δ_L , Δ_H in the four cases introduced previously.

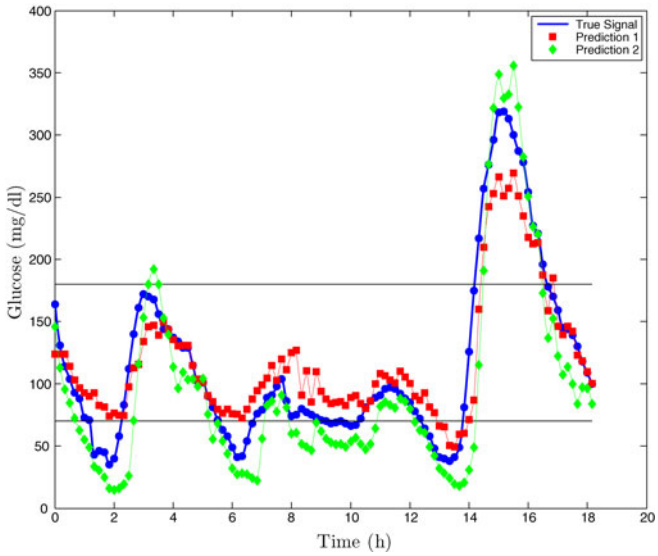

Fig. 8. CGM profile of subject #3 collected during the first admission of the study [26], held in Padova, Italy, in 2008. Two different predictions are shown. Prediction 1 has a smaller MSE but visual inspection suggests that prediction 2 should be preferred. This is well captured by gMSE, which is 7.3% larger in prediction 1 than in prediction 2.

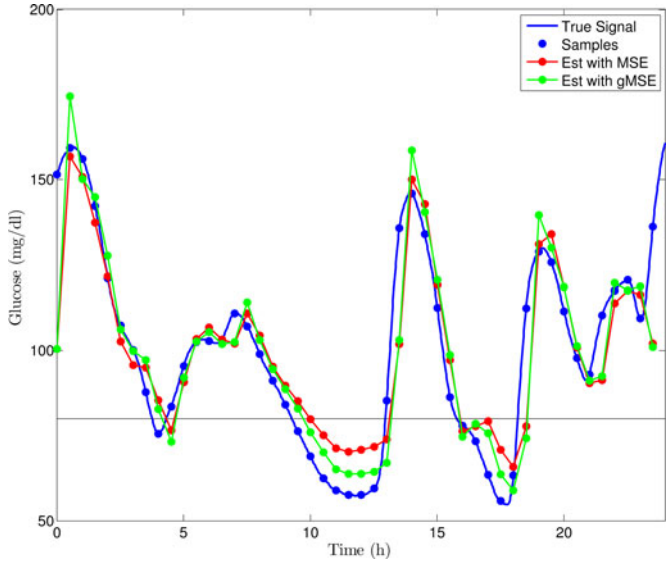

Fig. 9. True signal is obtained using UVA/Padova type-1 diabetic simulator [27]. The parameters of an ARX model are estimated minimizing either the MSE or the gMSE. The gMSE cost function increases model accuracy in the hyporegion.

Here we assume

$$g(t) = 125 + 85\sin(2\pi t)$$

therefore, $g(t) \in [40,\ 210]$, spending time both in hypo- and hyperglycemia. We consider the following four situations.

1) *Hypo- and hyperamplification:* $\Delta_L \in [-100\%,\ 0]$ and $\Delta_H = -\Delta_L = [0,\ 100\%]$. This is the less dangerous combination since both in hypo and in hyper the intensity of an episode is overestimated.
2) *Hypoamplification and hyperattenuation:* $\Delta_L \in [-100\%,\ 0]$ and $\Delta_H = \Delta_L = [-100\%,\ 0]$. In this case, the intensity of hypoepisodes is overestimated, while the intensity of hyperepisodes is underestimated. This situation is therefore more dangerous than the first one.
3) *Hypoattenuation and hyperamplification:* $\Delta_L \in [0,\ 100\%]$ and $\Delta_H = \Delta_L = [0,\ 100\%]$. In this case, the intensity of hyper episodes is overestimated, while the intensity of hypoepisodes is underestimated. This situation is therefore more dangerous than both previous two.
4) *Hypo- and hyperattenuation:* $\Delta_L \in [0,\ 100\%]$ and $\Delta_H = -\Delta_L = [-100\%,\ 0]$. This is the most dangerous combination since both in hypo and in hyper the intensity of an episode is underestimated.

In Fig. 7, the cost function values are plotted against the hypo- and hyperglycemic distortions Δ_L , Δ_H in the four situations mentioned previously. MSE is not able to exhibit different sensitivity in the different situations, being based only on the error norm. On the contrary, the new gMSE inherits the fine sensitivity of the quadratic error function but shows an increased sensitivity in the dangerous situations: in Fig. 7(c), one can notice that when hyperintensity is attenuated and hypo is amplified (yellow line), the cost function value increases more rapidly then when both hypo and hyper are overestimated (green line), but less rapidly then when hypo intensity is underestimated and hyper overestimated, a more dangerous situation (orange line). Finally, we note that the fastest increase is in the most dangerous case, both hypo- and hyperattenuated (red line).

TABLE II
DEFINITION OF MAD, MARD, AND COD AND THEIR EXTENSION FOR DIABETES CARE PURPOSES (SEE FOOTNOTE[3]). $\bar{g}$ DENOTES $\bar{g} = \frac{1}{N}\sum_{t=1}^{N} g(t)$

MAD	MARD	CoD
$\frac{1}{N}\sum_{t=1}^{N}\lvert g(t)-\hat{g}(t)\rvert$	$\frac{1}{N}\sum_{t=1}^{N}\frac{\lvert g(t)-\hat{g}(t)\rvert}{g(t)}$	$1-\frac{\frac{1}{N}\sum_{t=1}^{N}\lvert g(t)-\hat{g}(t)\rvert^2}{\frac{1}{N}\sum_{t=1}^{N}\lvert g(t)-\bar{g}\rvert^2}$
gMAD	**gMARD**	**gCoD**
$\frac{1}{N}\sum_{t=1}^{N} Pen\Big(g(t),\hat{g}(t)\Big)\Big\lvert g(t)-\hat{g}(t)\Big\rvert$	$\frac{1}{N}\sum_{t=1}^{N}\frac{Pen\Big(g(t),\hat{g}(t)\Big)\Big\lvert g(t)-\hat{g}(t)\Big\rvert}{g(t)}$	$1-\frac{\frac{1}{N}\sum_{t=1}^{N} Pen\Big(g(t),\hat{g}(t)\Big)\Big\lvert g(t)-\hat{g}(t)\Big\rvert^2}{\frac{1}{N}\sum_{t=1}^{N} Pen\Big(g(t),\bar{g}\Big)\Big\lvert g(t)-\bar{g}\Big\rvert^2}$

TABLE III
PREDICTION ASSESSMENT METRIC USED TO CHOOSE AMONG PREDICTIONS 1 AND 2 IN THE EXAMPLE OF SECTION V

	MSE	MAD	MARD	CoD	gMSE	gMAD	gMARD	gCOD
Prediction 1	**702.4**	**20.6**	**0.2384**	**61.99%**	1197.6	34.85	0.4473	87.32%
Prediction 2	997.8	23.3	0.2422	54.70%	**1116.1**	**24.76**	**0.2486**	**88.19%**

All general purpose metrics fail to select prediction 2, which is preferable on a clinical point of view.
On the contrary, all their glucose-specific counterparts select prediction 2.

V. PREDICTION ASSESSMENT CASE STUDY

In this section, we consider the CGM profile of subject #3 collected during the first admission of a Juvenile Diabetes Research Foundation (JDRF) study held in Padova, Italy, in 2008, see [26] for reference and details on the experiment. The profile is reported in Fig. 8 (blue line). We computed two different predictions of future glycemic concentrations using a prediction horizon of 30 min, depicted in red (prediction 1) and green (prediction 2) in Fig. 8. [1]Predictor 1 has an MSE of approximatively 702.5 while predictor 2 has an MSE of approximatively 997.8, 42% lager than prediction 1. Therefore, using MSE as a selection criterion, the first prediction should be chosen. However, a number of clinical considerations suggest that the second prediction is preferable. First of all, prediction 2 successfully predicts all the hypoglicemic episodes, while prediction 1 fails in predicting those at times $t = 1.5, 6$, and 10 h. Moreover, in the time interval $t = 8 - 12$ h, prediction 1 overestimates the measured glucose concentration, which is close to the hypoglycemic zone, while prediction 2 underestimates it, calling for patient attention to the episode. Finally, prediction 1 underestimates the hyperglycemic episode while prediction 2 is fairly accurate. In view of these considerations, prediction 2 is preferable from a clinical perspective. Looking at values obtained using the gMSE metric, prediction 2 has gMSE $\cong 1116.1$ while prediction 1 has gMSE $\cong 1197.6$, 7.3% more than prediction 2. Therefore, the use of the gMSE as a selection criterion would allow choosing the prediction that can be considered clinically more suitable, i.e., prediction 2.

VI. MODEL IDENTIFICATION CASE STUDY

In this section, we consider a realistic profile $y(t)$, obtained using University of Virginia (UVa)/Padova type-1 diabetic simulator [27], as reported in Fig. 9 (blue line). From a clinical point of view, the patient has a suboptimal glycemic control, facing significant hypoepisodes. Fifty very accurate samples are recorded, as shown Fig. 9 (blue circles). An ARX model of order 3[2] is estimated from the profile, minimizing either MSE or gMSE cost. The overall fit is rather poor since we have only few degree of freedom to follow a very complicate pattern. However, Fig. 9 shows that the gMSE (green stars) forces the use of the degrees of freedom to obtain a model that is more accurate in hypoglycemia. Having only limited degrees of freedom, it is a little less accurate than MSE-chosen model in euglycemia region. On the contrary, the MSE model uses the degrees of freedom to achieve the same accuracy in both eu- and hypoglycemia region. From a clinical perspective, the model identified by gMSE is preferable.

VII. OTHER PREDICTION ASSESSMENT METRICS

MSE is probably the most used loss function for system identification routines, but when considering glucose prediction assessment, a number of other metrics are sometimes used in place of MSE, for instance, mean absolute difference (MAD), mean absolute relative difference (MARD), and CoD, whose definitions are recalled in Table II.[3] As for the case of MSE, all these metrics are not designed specifically for diabetes application. In fact, they all penalize the absolute value of the error $|g - \hat{g}|$ only, without taking into account error's sign and glucose value g. As demonstrated in this paper, this information can be extremely relevant in a clinical perspective. Also MAD, MARD, and CoD can be modified and improved exploiting the penalty function Pen, defined in (2), and applying the same rationale used for the definition of gMSE . In Table II, we introduce gMAD, gMARD, and gCoD, the glucose specific alternative to the generic purpose metrics. Their effectiveness can be shown using analogous experiments to those reported in Sections IV and V for gMSE, but due to space limitations, we defer an extensive comparison to future work. However, it is interesting to see which is

[1]A detailed description of the techniques used to obtain the predictors is not significant for the purposes of the example and fall beyond the scope of this paper. We just mention here that they relay on simple autoregressive models. Similar results can be achieved using a different prediction horizon.

[2]Analogous results are obtained using other orders.

[3]Note that the best prediction has the smallest MSE, MAD, MARD, but the greatest CoD. The same holds for the glucose-specific counterparts.

the assessment given by MAD, MARD, and CoD on the example reported in Section V, see Table III. Note that all the general purpose metrics fail to detect prediction 2 as the preferable. On the contrary, all their glucose-specific counterparts, gMAD, gMARD and gCoD, select prediction 2.

VIII. Conclusion

In this paper, we have proposed a new glucose-oriented cost function with a two-fold purpose: first, to assess the accuracy of a predicted glucose profile from a clinical perspective, and second, to use it in place of MSE in model identification.

We have shown how MSE is not fully satisfactory when used to assess glucose predictions in diabetes applications. In fact, relying only on the absolute error, MSE weights equally situations with the same absolute prediction error, while these situations may present different harmful risks, for instance, eu- and hypoglycemia.

To overcome this, we have developed a gMSE, which has the advantage of taking into account also the clinical impact of prediction error. In practice, we have modified the original MSE with a CEG-inspired penalty function, which penalizes overestimation in hypoglycemia and underestimation in hyperglycemia, which are the most harmful situations.

In support of our choice, we have presented three thought experiments, designed to test the new metric sensitivity to prediction accuracy, precision, and distortion. Results show that the new cost function retains fine sensitivity of MSE and manages to distinguish between differently dangerous clinical conditions, by exhibiting as increased sensitivity specifically in potentially harmful conditions. Moreover, we have compared the new metric and MSE in the assessment of prediction obtain from real data, obtaining the same qualitative indications achieved in thought experiments.

Finally, we have proved that the new metric inherits MSE convexity, implying that it has no local minima. This makes the new metric suitable to be used in place of MSE as cost function in model identification. Model identification algorithms are then forced to spend the available degrees of freedom to derive models that are especially accurate in potentially harmful situations (hypo- and hyperglycemia), as we illustrated through a simulation example.

Besides MSE, other prediction assessment metrics have been considered, illustrating how the same rationale used to design gSE can be applied in other cases also, allowing to take into account clinically relevant information otherwise unconsidered.

Appendix A
Sigmoidal Functions

The sigmoid-like functions, σ and $\bar{\sigma}$ are defined as follows:

$$\sigma_{x\geq a,\epsilon}(x)=\begin{cases}0, & \text{if} \quad x\leq a\\ -\frac{1}{2}\xi^4-\xi^3+\xi+\frac{1}{2}, & \text{if} \quad a\leq x\leq a+\epsilon/2\\ \frac{1}{2}\xi^4-\xi^3+\xi+\frac{1}{2}, & \text{if} \quad a+\epsilon/2\leq x\leq a+\epsilon\\ 1, & \text{if} \quad a+\epsilon\leq x\end{cases}$$

$$\bar{\sigma}_{x\leq a,\epsilon}(x)=\begin{cases}1, & \text{if} \quad x\leq a-\epsilon\\ \frac{1}{2}\bar{\xi}^4-\bar{\xi}^3+\bar{\xi}+\frac{1}{2}, & \text{if} \quad a-\epsilon\leq x\leq a-\epsilon/2\\ -\frac{1}{2}\bar{\xi}^4-\bar{\xi}^3+\bar{\xi}+\frac{1}{2}, & \text{if} \quad a-\epsilon/2\leq x\leq a\\ 0, & \text{if} \quad a\leq x\end{cases}$$

where we define

$$\xi:=\frac{2}{\epsilon}\left(x-a-\frac{2}{\epsilon}\right) \quad \text{and} \quad \bar{\xi}:=-\frac{2}{\epsilon}\left(x-a+\frac{2}{\epsilon}\right).$$

One can easily verify that both σ and $\bar{\sigma}$ are $\mathcal{C}^2$ functions, i.e., they are continuous functions with continuous first and second derivatives.

Appendix B
Proof of gSE Properties

In this section, we briefly report proof of Proposition 3.1. The proof is based on direct computation. Recall that

$$\mathrm{gSE}(g,\hat{g})=(g-\hat{g})^2\Bigg(1+\underbrace{\alpha_L\bar{\sigma}_{g\leq 85,\beta_L}(g)}_{\bar{\alpha}_L}\sigma_{\hat{g}\geq g,\gamma_L}(\hat{g},g)+\underbrace{\alpha_H\sigma_{g\geq 155,\beta_H}(g)}_{\bar{\alpha}_H}\bar{\sigma}_{\hat{g}\leq g,\gamma_H}(\hat{g},g)\Bigg)$$

and note that $\bar{\alpha}_L=0$ for all $g\geq 85$ while $\bar{\alpha}_H=0$ for all $g\leq 155$.

Therefore, for $85\leq g\leq 155$:

$$\mathrm{gSE}(g,\hat{g})=(g-\hat{g})^2 \quad \Rightarrow \quad \frac{\partial^2}{\partial\hat{g}^2}\mathrm{gSE}(g,\hat{g})=2>0.$$

Let us consider now that $g<85$. Hence, $0<\bar{\alpha}_L\leq\alpha_L$ while $\bar{\alpha}_H=0$. Recalling the definition of σ, one has that if $g>\hat{g}$ again

$$\mathrm{gSE}(g,\hat{g})=(g-\hat{g})^2 \quad \Rightarrow \quad \frac{\partial^2}{\partial\hat{g}^2}\mathrm{gSE}(g,\hat{g})=2>0$$

while if $g+\gamma_L<\hat{g}$, then $\mathrm{gSE}(g,\hat{g})=(g-\hat{g})^2(1+\bar{\alpha}_L)$

$$\Rightarrow \frac{\partial^2}{\partial\hat{g}^2}\mathrm{gSE}(g,\hat{g})=2(1+\bar{\alpha}_L)>0.$$

Consider then the case $g\leq\hat{g}\leq g+\gamma_L/2$. One can easily check that

$$\frac{\partial^2}{\partial\hat{g}^2}\mathrm{GSE}(g,\hat{g})=2\left(1+\bar{\alpha}_L\sigma_{\hat{g}\geq g,\gamma_L}(\hat{g},g)\right) \tag{4}$$

$$-2(g-\hat{g})\left(1+\bar{\alpha}_L\frac{\partial}{\partial\hat{g}}\sigma_{\hat{g}\geq g,\gamma_L}(\hat{g},g)\right) \tag{5}$$

$$+(g-\hat{g})^2\left(1+\bar{\alpha}_L\frac{\partial^2}{\partial\hat{g}^2}\sigma_{\hat{g}\geq g,\gamma_L}(\hat{g},g)\right). \tag{6}$$

Note that σ is always positive and monotonically increasing

$$\sigma_{\hat{g}\geq g,\gamma_L}(\hat{g},g)\geq 0, \qquad \frac{\partial}{\partial\hat{g}}\sigma_{\hat{g}\geq g,\gamma_L}(\hat{g},g)>0.$$

Note moreover that when $g \leq \hat{g} \leq g + \gamma_L/2$, σ is also convex, i.e.,

$$\frac{\partial^2}{\partial \hat{g}^2} \sigma_{\hat{g} \geq g, \gamma_L}(\hat{g}, g) > 0$$

therefore, for $g \leq \hat{g} \leq g + \gamma_L/2$, it is easy to see that three terms (4)–(6) are all positive, and hence the second derivative is positive.

When $g + \gamma_L/2 \leq \hat{g} \leq g + \gamma_L$, the function σ is concave and therefore we are forced to carry out the exact computations, which tediously lead to

$$\frac{\partial^2}{\partial \hat{g}^2} \mathrm{gSE}(g, \hat{g}) = 2 + \bar{\alpha}_L \left(15\xi^4 - 18\xi^2 + 5 \right)$$

where $\xi = \frac{2}{d}(\hat{g} - g - d/2)$. $0 < \xi < 1$ when $g + \gamma_L/2 \leq \hat{g} \leq g + \gamma_L$. It can be easily shown that the minimum of $15\xi^4 - 18\xi^2 + 5$ is $-2/5$ for $0 < \xi < 1$, therefore,

$$\frac{\partial^2}{\partial \hat{g}^2} \mathrm{gSE}(g, \hat{g}) > 2 - \frac{2}{5}\bar{\alpha}_L > 2 - \frac{2}{5}\alpha_L.$$

If $\alpha_L < 5$, this implies that $\frac{\partial^2}{\partial \hat{g}^2} > 0$.

Analogous arguments are used to study the case $g \geq 155$. □

ACKNOWLEDGMENT

The authors would like to thank Dr. G. Pillonetto and Prof. G. Sparacino, both with the Department of Information Engineering, University of Padova, Padova, Italy, for invaluable discussions on the topic.

REFERENCES

[1] T. Battelino and J. Bolinder, "Clinical use of real-time continuous glucose monitoring," *Curr. Diabetes Rev.*, vol. 4, pp. 218–222, Aug. 2008.

[2] I. B. Hirsch, J. Abelseth, B. W. Bode, J. S. Fischer, F. R. Kaufman, J. Mastrototaro, C. G. Parkin, H. A. Wolpert, and B. A. Buckingham, "Sensor-augmented insulin pump therapy: Results of the first randomized treat-to-target study," *Diabetes Technol. Ther.*, vol. 10, pp. 377–383, Oct. 2008.

[3] D. C. Klonoff, "Continuous glucose monitoring: Roadmap for 21st century diabetes therapy," *Diabetes Care*, vol. 28, pp. 1231–1239, May 2005.

[4] C. Cobelli, C. Dalla Man, G. Sparacino, L. Magni, G. De Nicolao, and B. P. Kovatchev, "Diabetes: Models, signals, and control," *IEEE Rev. Biomed. Eng.*, vol. 2, pp. 54–96, Jan. 2009.

[5] R. Hovorka, "The future of continuous glucose monitoring: Closed loop," *Curr. Diabetes Rev.*, vol. 4, pp. 269–279, Aug. 2008.

[6] G. Sparacino, A. Facchinetti, and C. Cobelli, "Smart continuous glucose monitoring sensors: On-line signal processing issues," *Sensors*, vol. 10, pp. 6751–6772, 2010.

[7] B. Buckingham, E. Cobry, P. Clinton, V. Gage, K. Caswell, E. Kunselman, F. Cameron, and H. P. Chase, "Preventing hypoglycemia using predictive alarm algorithms and insulin pump suspension," *Diabetes Technol. Ther.*, vol. 11, pp. 93–97, Feb. 2009.

[8] E. Dassau, F. Cameron, H. Lee, B. W. Bequette, H. Zisser, L. Jovanovic, H. P. Chase, D. M. Wilson, B. A. Buckingham, and F. J. Doyle, "Real-time hypoglycemia prediction suite using continuous glucose monitoring: A safety net for the artificial pancreas," *Diabetes Care*, vol. 33, pp. 1249–1254, Jun. 2010.

[9] J. B. Rawlings and D. Q. Mayne, *Model Predictive Control Theory and Design*. San Francisco, CA: Nob Hill, 2009.

[10] C. Cobelli, C. Dalla Man, G. Sparacino, L. Magni, G. De Nicolao, and B. Kovatchev, "Diabetes: Models, signals and control," *IEEE Rev. Biomed. Eng.*, vol. 2, pp. 54–96, 2009.

[11] C. Cobelli, E. Renard, and B. Kovatchev, "Artificial pancreas: Past, present, future," *Diabetes*, vol. 60, pp. 2672–2682, Nov. 2011.

[12] R. Hovorka, L. J. Chassin, M. E. Wilinska, V. Canonico, J. A. Akwi, M. O. Federici, M. Massi-Benedetti, I. Hutzli, C. Zaugg, H. Kaufmann, M. Both, T. Vering, H. C. Schaller, L. Schaupp, M. Bodenlenz, and T. R. Pieber, "Closing the loop: The adicol experience," *Diabetes Technol. Ther.*, vol. 6, pp. 307–318, Jun. 2004.

[13] M. E. Wilinska, L. J. Chassin, and R. Hovorka, "In silico testing-impact on the progress of the closed loop insulin infusion for critically ill patients project," *J. Diabetes Sci. Technol.*, vol. 2, pp. 417–423, May 2008.

[14] G. Sparacino, F. Zanderigo, S. Corazza, A. Maran, A. Facchinetti, and C. Cobelli, "Glucose concentration can be predicted ahead in time from continuous glucose monitoring sensor time-series," *IEEE Trans. Biomed. Eng.*, vol. 54, no. 5, pp. 931–937, May 2007.

[15] C. Perez-Gandia, A. Facchinetti, G. Sparacino, C. Cobelli, E. J. Gomez, M. Rigla, A. de Leiva, and M. E. Hernando, "Artificial neural network algorithm for online glucose prediction from continuous glucose monitoring," *Diabetes Technol. Ther.*, vol. 12, pp. 81–88, Jan. 2010.

[16] S. M. Pappada, B. D. Cameron, P. M. Rosman, R. E. Bourey, T. J. Papadimos, W. Olorunto, and M. J. Borst, "Neural network-based real-time prediction of glucose in patients with insulin-dependent diabetes," *Diabetes Technol. Ther.*, vol. 13, pp. 135–141, Feb. 2011.

[17] A. Gani, A. V. Gribok, Y. Lu, W. K. Ward, R. A. Vigersky, and J. Reifman, "Universal glucose models for predicting subcutaneous glucose concentration in humans," *IEEE Trans. Inf. Technol. Biomed.*, vol. 14, no. 1, pp. 157–165, Jan. 2010.

[18] S. Del Favero, G. Pillonetto, C. Cobelli, and G. De Nicolao, "A novel nonparametric approach for the identification of the glucose-insulin systemin Type 1 diabetic patients," in *Proc. 18th IFAC World Congr.*, 2011, p. 4. DOI: 10.3182/20110828-6-IT-1002.01929.

[19] L. Ljung, *System Identification—Theory For the User*, 2nd ed. ed. Upper Saddle River, NJ: PTR Prentice-Hall, 1999.

[20] W. L. Clarke, D. Cox, L. A. Gonder-Frederick, W. Carter, and S. L. Pohl, "Evaluating clinical accuracy of systems for self-monitoring of blood glucose," *Diabetes Care*, vol. 10, pp. 622–628, 1987.

[21] A. Facchinetti, G. Sparacino, E. Trifoglio, and C. Cobelli, "A new index to optimally design and compare continuous glucose monitoring glucose prediction algorithms," *Diabetes Technol. Ther.*, vol. 13, pp. 111–119, Feb. 2011.

[22] M. Cescon and R. Johansson, "Glycemic trend prediction using empirical model identification," in *Proc. Joint 48th CDC*, 2009, pp. 3501–3506.

[23] D. Finan, C. Palerm, F. Doyle III, D. Seborg, H. Zisser, W. Bevier, and L. Jovanovic, "Effect of input excitation on the quality of empirical dynamic models for type 1 diabetes," *AIChE J.*, vol. 55, pp. 1135–1146, 2009.

[24] B. Kovatchev, S. Anderson, L. Heinemann, and W. Clarke, "Comparison of the numerical and clinical accuracy of four continuous glucose monitors," *Diabetes Care*, vol. 31, pp. 1160–1164, Jun. 2008.

[25] S. K. Garg, J. Smith, C. Beatson, B. Lopez-Baca, M. Voelmle, and P. A. Gottlieb, "Comparison of accuracy and safety of the SEVEN and the Navigator continuous glucose monitoring systems," *Diabetes Technol. Ther.*, vol. 11, pp. 65–72, Feb. 2009.

[26] B. Kovatchev, C. Cobelli, E. Renard, S. Anderson, M. Breton, S. Patek, W. Clarke, D. Bruttomesso, A. Maran, S. Costa, A. Avogaro, C. Dalla Man, A. Facchinetti, L. Magni, G. De Nicolao, J. Place, and A. Farret, "Multinational study of subcutaneous model-predictive closed-loop control in type 1 diabetes mellitus: summary of the results," *J. Diabetes Sci. Technol.*, vol. 4, pp. 1374–1381, 2010.

[27] B. Kovatchev, M. Breton, C. Cobelli, and C. Dalla Man, "Method, system and computer simulation environment for testing of monitoring and control strategies in diabetes," Patent WO/2008/157781, 2008.

Simone Del Favero was born in Pieve di Cadore (BL), Italy, on November 7, 1982. He received the Doctoral degree (Laurea) cum laude in automation engineering and the Ph.D. degree in information science and technology from the University of Padova, Padova, Italy, in 2006, and March 2010, respectively.

He is currently a Postdoctoral Researcher at the University of Padova and he works within an international team to the designing, development, and clinical testing of minimally invasive artificial pancreas based on subcutaneous glucose sensing and subcutaneous insulin infusion. His research interests include estimation, learning and dynamical system identification, with applications to sensor networks and physiological systems, especially the insulin–glucose system.

Andrea Facchinetti was born in Padova, Italy, on July 27, 1981. He received the Doctoral degree (Laurea) cum laude in information engineering and the Ph.D. degree in bioengineering from the University of Padova, Padova, Italy, in 2005 and 2009, respectively.

He is currently a Postdoctoral Researcher at the University of Padova. He is the author or coauthor of more than 15 papers in international peer-reviewed journals. His current scientific research interests include optimal filtering, Bayesian estimation, deconvolution techniques, neural networks applied to signal processing problems, and bioinformatics techniques applied to predict functional annotations of gene products.

Claudio Cobelli (S'67–M'70–SM'97–F'03) was born in Bressanone (Bolzano), Italy, on February 21, 1946. He received the Doctoral degree (Laurea) in electrical engineering from the University of Padova, Padova, Italy, in 1970.

From 1970 to 1980, he was a Research Fellow at the Institute of System Science and Biomedical Engineering, National Research Council, Padova. From 1973 to 1975 and 1975 to 1981, he was an Associate Professor of Biological Systems at the University of Florence and an Associate Professor of Biomedical Engineering at the University of Padova, where he has been a Full Professor of Biomedical Engineering since 1981, and a Chairman of the Ph.D. Program in Bioengineering since 2000. Since 2000, he has been an Affiliate Professor of Bioengineering at the University of Washington, Seattle, WA. From 2000 to 2009, he has been Chairman of the Graduate Program in Biomedical Engineering. He is the author or coauthor of more than 300 papers in internationally refereed journals. He is a coeditor of *Carbohydrate Metabolism: Quantitative Physiology and Mathematical Modeling* (Chichester, U.K.: Wiley, 1981), *Modeling and Control of Biomedical Systems* (Oxford, U.K.: Pergamon, 1989) and *Modeling Methodology for Physiology and Medicine* (New York: Academic Press, 2000). He is a coauthor of *The Mathematical Modeling of Metabolic and Endocrine Systems* (New York: Wiley, 1983), *Tracer Kinetics in Biomedical Research: From Data to Model* (London, U.K.: Kluwer Academic/Plenum Publishers, 2001), and *Introduction to Modeling in Physiology and Medicine* (San Diego, CA: Academic, 2008). His research interests include the modeling and identification of physiological systems, especially endocrine–metabolic systems.

Dr. Cobelli is currently an Associate Editor of the IEEE TRANSACTION ON BIOMEDICAL ENGINEERING. He is on the Editorial Board of the American Journal of Physiology: Endocrinology and Metabolism, and of Journal of Diabetes Science & Technology. In the past, he has been an Associate Editor of Mathematical Biosciencies and on the Editorial Board of Control Engineering Practice; Diabetes, Nutrition & Metabolism; Diabetologia; and the American Journal of Physiology: Modeling in Physiology. He has been a Chairman of the Italian Biomedical Engineering Group (1999–2004), Chairman of IFAC TC on Modeling and Control of Biomedical Systems (1990–1993 and 1993–1996), and IEEE Engineering in Medicine and Biology Society AdCom Member (2008–2009). In 2010, he received the Diabetes Technology Artificial Pancreas Research Award. He is a Fellow of the Biomedical Engineering Society and the American Institute for Medical and Biological Engineering.